Late-time tails of a self-gravitating Einstein-Skyrme model

Stanisław Zając[1]

[1] *H. Niewodniczanski Institute of Nuclear Physics, Polish Academy of Sciences, Kraków, Poland*

(Dated: January 26, 2010)

We consider the long-time behaviour of spherically symmetric solutions in the Einstein-Skyrme model. Using *nonlinear* perturbation analysis we obtain the leading order estimation of the tail in the topologically trivial sector ($B = 0$) of the model. We showed that solutions starting from small compactly supported initial data decay as t^{-4} at future timelike infinity and as u^{-2} at future null infinity.

I. INTRODUCTION

This paper concerns the late-time asymptotic behaviour of a spherically symmetric self-gravitating Einstein-Skyrme (ES) model. It is an extension of the paper [2] where we studied quasinormal modes in intermediate asymptotics. It is also an extension of work done in [3] where the expression for the tail in flat space was obtained. The results of this paper are closely connected to the results of paper [4] where the evolution of wave maps was studied. As we remarked in paper [2], in gravitating Skyrme model the linear perturbation method predicts power-law index $\gamma = 5$ for the tail. This estimation is in clear conflict with early numerical results on tails in ES [1] which were later confirmed by the results of paper [2]. To explain this disagreement we have studied the expression for the tail in gravitating wave maps [4] model where we expected similar long-time asymptotics as for the Skyrme model. In the current paper direct calculations in gravitating Skyrme model are performed.

In self–gravitating Skyrme model the most interesting problem is certainly the description of the relaxation to the static Skyrmion. Unfortunately, due to the lack of analytic formulae describing static Skyrme soliton, the description of this problem is very tedious. To avoid these difficulties we follow [3] and study the relaxation to the vacuum in the topologically trivial $B = 0$ sector. To estimate the parameters of the tail we apply perturbation techniques elaborated in [5–8]. Using these techniques we will demonstrate that the third-order expression for the tail agrees perfectly with numerical results for small initial data. The plan of this paper is as follows. In section II we remind the reader the field equations of the model and shortly demonstrate the iterative scheme. Section III contains the details of perturbation calculations. In the last section we demonstrate the numerical evidence confirming our analytical estimations for the tails.

II. THEORETICAL BACKGROUND

We consider the Einstein–Skyrme model with dynamics given by the Lagrangian [9]:

$$L = \frac{f^2}{4} Tr(\nabla_a \nabla^a U^{-1}) + \frac{1}{32e^2} Tr[(\nabla_a U)U^{-1}, (\nabla_b U)U^{-1}]^2 - \frac{1}{16\pi G} R. \tag{1}$$

We assume spherical symmetry and parametrize the metric as follows:

$$ds^2 = -e^{-2\delta(r,t)} N(r,t) dt^2 + N^{-1}(r,t) dr^2 + r^2 d\Omega^2, \tag{2}$$

where $d\Omega^2$ is a metric on the unit 2–sphere. Applying the standard hedgehog ansatz $U = exp(i\overrightarrow{\sigma} \cdot \hat{r} F(r,t))$, where $\overrightarrow{\sigma}$ is the vector of Pauli matrices and $\hat{r}$ – unit radial vector, we obtain the following set of ES equations:

$$\dot{m} = \alpha e^{-\delta} N^2 P F', \tag{3}$$

$$m' = \frac{\alpha}{2} \left(2\sin^2 F + \frac{\sin^4 F}{r^2} + uN(\frac{P^2}{u^2} + F'^2) \right), \tag{4}$$

$$\delta' = -\frac{\alpha u}{r} \left(\frac{P^2}{u^2} + F'^2 \right), \tag{5}$$

$$\dot{P} = (e^{-\delta} N u F')' + \sin(2F) e^{-\delta} \left(N(\frac{P^2}{u^2} - F'^2) - \frac{\sin^2 F}{r^2} - 1 \right). \tag{6}$$

Here P and u are auxiliary variables defined as: $P = ue^{\delta}N^{-1}\dot{F}$ and $u = r^2 + 2\sin^2 F$, $m(t,r)$ is the mass function defined as: $m(t,r) = \frac{r(1-N)}{2}$ and $\alpha = 4\pi G f^2$ is dimensionless coupling constant. The expression for the tail for $\alpha = 0$ (flat space) was obtained in paper [3]; here we consider gravitating case $\alpha > 0$.

To obtain the estimation of the tail we study the evolution of the system described by (3-6) starting with small, smooth and compactly supported initial data

$$F(0,r) = \varepsilon f(r), \qquad \dot{F}(0,r) = \varepsilon g(r)\,. \tag{7}$$

Following [5–8] we postulate perturbation expansion

$$\begin{aligned} m(t,r) &= m_0(t,r) + \varepsilon m_1(t,r) + \varepsilon^2 m_2(t,r) + \ldots, &(8)\\ \delta(t,r) &= \delta_0(t,r) + \varepsilon \delta_1(t,r) + \varepsilon^2 \delta_2(t,r) + \ldots, &(9)\\ F(t,r) &= F_0(t,r) + \varepsilon F_1(t,r) + \varepsilon^2 F_2(t,r) + \varepsilon^3 F_3(t,r) + \ldots. &(10)\end{aligned}$$

Collecting the terms with the same power of ε we obtain a set of equations for the expansion functions which we solve recursively. We are studying the relaxation process to the Minkowski space-time, so $m_0 = \delta_0 = F_0 = 0$.

In the first order in ε the requirement of regularity of the metric function N at the origin and choice of gauge $\delta(t, r = 0) = 0$ require that $m_1 = \delta_1 = 0$. In this perturbation order we obtain free $\ell = 1$ radial wave equation for the F_1 function:

$$\Box F_1 = 0\,, \qquad \Box = \partial_t^2 - \partial_r^2 - \frac{2}{r}\partial_r + \frac{2}{r^2}\,, \tag{11}$$

with initial data $F_1(0,r) = f(r), \dot{F}_1(0,r) = g(r)$. The general regular solution of an equation of this kind has the form

$$F_1(t,r) = \frac{a'(t-r) + a'(t+r)}{r} + \frac{a(t-r) - a(t+r)}{r^2}\,. \tag{12}$$

where the generating function $a(r)$ is determined by initial data.

In the second perturbation order we obtain the free $\ell = 1$ radial wave equation $\Box F_2 = 0$; however, contrary to the previous $F_1(t,r)$ case, the initial data for F_2 are zero so F_2 has to vanish. In this order of perturbation expansion, the metric functions satisfy the following equations

$$\begin{aligned} m_2' &= \frac{\alpha}{2} r^2 \left(\dot{F}_1^2 + F_1'^2 + \frac{2}{r^2}F_1^2\right), &(13)\\ \dot{m}_2 &= \alpha\, r^2\, \dot{F}_1\, F_1', &(14)\\ \delta_2' &= -\alpha\, r\, (\dot{F}_1^2 + F_1'^2)\,. &(15)\end{aligned}$$

Finally in the third order in ε we get following equation for F_3

$$\begin{aligned} \Box F_3 &= -2\delta_2 \ddot{F}_1 - \dot{\delta}_2 \dot{F}_1 - \delta_2' F_1' - \frac{2}{r}\left(m_2' F_1' + \dot{m}_2 \dot{F}_1\right) + \frac{m_2}{r}\left(\frac{4}{r^2}F_1 - \frac{6}{r}F_1' - 4F_1''\right)\\ &+ \frac{4}{3r^2}F_1^3 + \frac{2}{r^4}\left(F_1^3 - 2rF_1^2\, F_1' + r^2\, F_1\, (F_1'^2 - \dot{F}_1^2)\right) \end{aligned} \tag{16}$$

To solve the above equation we use the Duhamel formula for the solution of the inhomogeneous wave equation $\Box_l F = N(t,r)$ with zero initial data

$$F(t,r) = \frac{1}{2r}\int_0^t d\tau \int_{|t-r-\tau|}^{t+r-\tau} \rho P_\ell(\mu) N(\tau,\rho) d\rho\,. \tag{17}$$

Here $P_\ell(\mu)$ are Legendre polynomials of degree ℓ and $\mu = (r^2 + \rho^2 - (t-\tau)^2)/2r\rho$. Using the abbreviation $K(m,\delta,F)$:

$$\begin{aligned} K(m,\delta,F) &= -2\delta \ddot{F} - \dot{\delta}\dot{F} - \delta' F' - \frac{2}{r}\left(m' F' + \dot{m}\dot{F}\right) + \frac{m}{r}\left(\frac{4}{r^2}F - \frac{6}{r}F' - 4F''\right)\\ &+ \frac{4}{3r^2}F^3 + \frac{2}{r^4}\left(F^3 - 2rF^2\, F' + r^2\, F\, (F'^2 - \dot{F}^2)\right), \end{aligned} \tag{18}$$

and introducing null coordinates: $\eta = \tau - \rho$ and $\xi = \tau + \rho$, we obtain:

$$F_3(t,r) = \frac{1}{8r}\int_{|t-r|}^{t+r} d\xi \int_{-\xi}^{t-r} (\xi - \eta) P_\ell(\mu) K(m_2(\xi,\eta), \delta_2(\xi,\eta), F_1(\xi,\eta)) d\eta\,, \tag{19}$$

where $\mu = (r^2 + (\xi - t)(t - \eta))/r(\xi - \eta)$.

We have assumed that the initial data $F_1(t,r)$ are compactly supported, i.e. they vanish outside a ball of some radius R. As a result, for $t > r + R$ we may drop the advanced part of $F_1(t,r)$. Changing the order of integration in (19) we get:

$$F_3(t,r) = \frac{1}{8r} \int\limits_{-\infty}^{\infty} d\eta \int\limits_{t-r}^{t+r} (\xi - \eta) P_\ell(\mu) K(m_2(\xi,\eta), \delta_2(\xi,\eta), F_1^{ret}(\xi,\eta))\, d\xi\,. \tag{20}$$

We are interested in late–time behaviour of $F_3(t,r)$, so we need to know the behaviour of the metric function δ_2 and the mass function m_2 along the light cones for large values of r. To calculate (20), we expand the function K in inverse powers of $\rho = (\xi - \eta)/2$ and use the following identity (see paper [8]):

$$\int\limits_{t-r}^{t+r} d\xi\, \frac{P_\ell(\mu)}{(\xi-\eta)^n} = (-1)^l \frac{2(n-2)^{\underline{\ell}}}{(2\ell+1)!!}\, \frac{r^{\ell+1}(t-\eta)^{n-\ell-2}}{[(t-\eta)^2 - r^2]^{n-1}}\, F\left(\begin{matrix} \frac{\ell+2-n}{2}, \frac{\ell+3-n}{2} \\ \ell + 3/2 \end{matrix} \,\middle|\, \left(\frac{r}{t-\eta}\right)^2 \right). \tag{21}$$

III. NONLINEAR TAIL

To obtain the expression for the tail we have to solve the equations (13)–(15). Neglecting the advanced part of F_1 and integrating (13), we get the following expression for m_2 valid for large times

$$m_2(t,r) \overset{t\geq R}{=} \alpha \int\limits_0^r \left[\left(a''(t-\rho)\right)^2 - \frac{3}{2}\partial_\rho \frac{\left(a'(t-\rho)\right)^2}{\rho} - 2\partial_\rho \frac{a(t-\rho)a'(t-\rho)}{\rho^2} + \mathcal{O}\left(\frac{1}{\rho^3}\right)\right] d\rho. \tag{22}$$

We need this expression for $m_2(t,r)$ along the light cone, so it is convenient to use the null coordinate $u = t - r$ instead of t. As a result we get:

$$m_2(u,r) \overset{r+u>R}{=} \alpha \left[\int\limits_u^\infty \left(a''(s)\right)^2 ds - \frac{3}{2r}\left(a'(u)\right)^2 - \frac{2}{r^2} a(u)a'(u) + \mathcal{O}\left(\frac{1}{r^3}\right)\right]. \tag{23}$$

Using the same line of argument as in the text above and exploiting the gauge condition $\delta_2(t, r=0) = 0$ we get the formula for δ_2

$$\begin{aligned} \delta_2(u,r) \overset{r+u>R}{=} -\alpha \Bigg[& 2\int\limits_u^\infty \left(\frac{(a''(s))^2}{r} + \frac{(s-u)(a''(s))^2}{r^2} + \frac{(s-u)^2(a''(s))^2}{r^3}\right) ds - 3\frac{(a'(u))^2}{r^2} \\ & - \frac{4}{r^3}(a(u)a'(u)) - \frac{5}{r^3}\int\limits_u^\infty (a'(s))^2 ds + \mathcal{O}\left(\frac{1}{r^4}\right)\Bigg]. \end{aligned} \tag{24}$$

In order to get a compact formula for late-time asymptotics we define the following auxiliary symbol for the integrals of the form (for non-negative integers a, b)

$$I_b^a(u) = \int\limits_u^\infty (s-u)^a \left(a^{(b)}(s)\right)^2 ds. \tag{25}$$

Using this notation we get the following equation for m_2 and it's derivatives:

$$m_2(u,r) \overset{r+u>R}{=} \alpha \left[I_2^0(u) - \frac{3}{2r}(a'(u))^2 - \frac{2}{r^2}(a(u)a'(u)) + \mathcal{O}\left(\frac{1}{r^3}\right)\right], \tag{26}$$

$$\dot{m}_2(u,r) \overset{r+u>R}{=} -\alpha \left[(a''(u))^2 + \frac{3}{r}(a'(u)a''(u)) + \frac{2}{r^2}\left((a'(u))^2 + a(u)a''(u)\right) + \mathcal{O}\left(\frac{1}{r^3}\right)\right], \tag{27}$$

$$m_2'(u,r) \overset{r+u>R}{=} \alpha \left[(a''(u))^2 + \frac{3}{r}(a'(u)a''(u)) + \frac{1}{r^2}\left(\frac{7}{2}(a'(u))^2 + 2a(u)a''(u)\right) + \mathcal{O}\left(\frac{1}{r^3}\right)\right]. \tag{28}$$

Similary, from (24) we obtain:

$$\delta_2(u,r) \stackrel{r+u>R}{=} -\frac{\alpha}{r}\left[2I_2^0(u)+\frac{1}{r}\left(2I_2^1(u)-3(a'(u))^2\right)+\frac{1}{r^2}\left(2I_2^2(u)-5I_1^0(u)-4a'(u)a(u)\right)+\mathcal{O}\left(\frac{1}{r^3}\right)\right], \tag{29}$$

$$\dot{\delta}_2(u,r) \stackrel{r+u>R}{=} \frac{\alpha}{r}\left[2(a''(u))^2+\frac{1}{r}\left(2I_2^0(u)+6a'(u)a''(u)\right)+\frac{1}{r^2}\left(4I_2^1(u)-(a'(u))^2+4a(u)a''(u)\right)+\mathcal{O}\left(\frac{1}{r^3}\right)\right], \tag{30}$$

$$\delta_2'(u,r) \stackrel{r+u>R}{=} -\frac{\alpha}{r}\left[2(a''(u))^2+\frac{6}{r}(a'(u)a''(u))+\frac{1}{r^2}\left(5(a'(u))^2+4a(u)a''(u)\right)+\mathcal{O}\left(\frac{1}{r^3}\right)\right]. \tag{31}$$

Substituting (26-31) into (18) and using the equation (20) we get:

$$\begin{aligned} F_3(t,r) &= \frac{4\alpha}{r}\int\limits_{-\infty}^{+\infty}d\eta\int\limits_{t-r}^{t+r}d\xi\,\frac{P_1(\mu)}{(\xi-\eta)^2}\left[\frac{d}{d\eta}\left(I_2^1(\eta)a''(\eta)\right)\right. \\ &- \left.\frac{1}{\xi-\eta}\left((a''(\eta))^2a(\eta)-\frac{d}{d\eta}A_1(\eta)\right)+\mathcal{O}\left(\frac{1}{(\xi-\eta)^2}\right)\right], \end{aligned} \tag{32}$$

where

$$A_1(\eta)=4I_2^1(\eta)a'(\eta)-I_2^0(\eta)a(\eta)+(2I_2^2(\eta)-5I_1^0(\eta))a''(\eta)\,. \tag{33}$$

To obtain the final form of the expression for the tail we perform the inner integral over ξ in (32) and using the identity (21) we get the asymptotic behavior which is valid for large retarded times u

$$F_3(t,r)=\frac{r}{(t^2-r^2)^2}\left[\alpha C_1+\mathcal{O}\left(\frac{1}{t}\right)\right], \tag{34}$$

where

$$C_1=\frac{8}{3}\int\limits_{-\infty}^{+\infty}\left(a''(s)\right)^2a(s)\,ds\,. \tag{35}$$

We would like to stress that if we compare the equations (32) and (34) with equations (34) and (36) obtained in the paper [4] we immediately see that the leading order expressions for the tails obtained in both models are exactly the same. This is the case even though nonlinear formulae for F_3 are different. However, as we have expected, these differences are not significant in the leading order.

Finally, from (34) we get the late–time tails at the future timelike infinity $F_3(t,r)\simeq\alpha C_1 r t^{-4}$ (for $r=const$ and $t\to\infty$) and future null inifinity $(rF_3)(v=\infty,u)\simeq\alpha C_1(2u)^{-2}$ (for $v=\infty$ and $u\to\infty$).

IV. NUMERICS

To verify analytical prediction for the tails obtained in the previous section we have performed numerical studies of long-time asymptotics in Einstein-Skyrme model. To do that we have solved numerically the equations (3-6) with initial data descibed below. For solving evolutional equations we have used method of lines with 5-point, fourth order accurate spatial discretization. We have solved the resulting ODE's with fourth order Runge-Kutta method. To solve the costraints, i.e. hamiltonian constrain (4) and slicing condition (5) we have also used fourth order Runge-Kutta method. Here we need the values of some functions out of the grid – we have obtained them using spline interpolation. To ensure regularity at the origin we impose the boundary conditions $F(t,r=0)\sim r$ and $P(t,r=0)\sim r$. To avoid the contamination of results by parts of the solution reflected from outer boundary we have used the size of the grid big enough, so the solution stops before the reflected signal reaches the observation point. Finally, to suppress the acumulation of round-off errors in late times we have used quadrupole precision. In our calculations we have used the initial data obtained from the following generating function (see(7-12)):

$$\varepsilon a(x)=\varepsilon\, exp(-x^2), \tag{36}$$

with different values of ϵ. For initial data of this kind we get the value for C_1 from the formula (35):

$$C_1=\frac{64}{9}\sqrt{\frac{\pi}{3}}\approx 7.2769, \tag{37}$$

In Fig.1 we plot $F(t,r)$ in self–gravitating Skyrme model with $\alpha = 0.03$ for three different values of ϵ. We see that on log-log plots the late-time tails are clearly seen as straight lines.

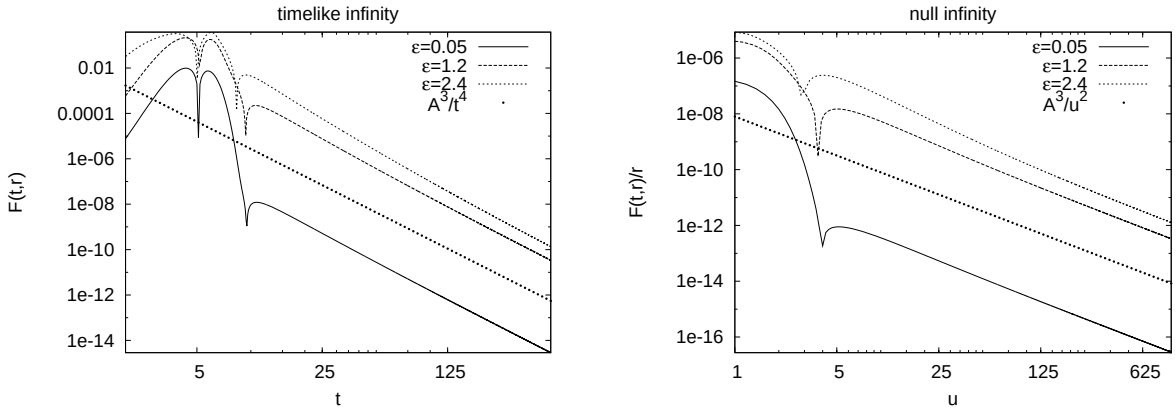

FIG. 1: Left panel: The log-log plot of $F(t,r)$ for fixed r=5. Right panel: The log-log plot of $F(t,r)/r$ for fixed large advanced time $v = t + r = 1000$ as the function of retarded time $u = t - r$. In both panels (dotted line) we see that solutions starting from small initial data decay as t^{-4} at future timelike infinity and as u^{-2} at future null infinity

To obtain the parameters of the tails i.e. the decay rate and the amplitude we fit numerical data with the formula:

$$F(t,r) = At^{-\gamma} \exp\left(B/t + C/t^2\right). \tag{38}$$

In Table 1 we present the numerical results for the decay rate and the amplitude and their comparison with analytic estimation.

Initial amplitude	*Theory (third order)*	*Numerics : F data*	*Numerics*
ε	A	A	γ
0.05	0.0001364	0.0001365	4.00
0.1	0.001091	0.001098	4.00
0.2	0.008732	0.008774	4.00
0.4	0.06985	0.06929	4.00
0.8	0.5589	0.5220	4.00
1.2	1.8862	1.5842	4.00
1.6	4.4709	3.1974	4.00
2.0	8.7324	4.9482	4.00
2.4	15.0896	6.3257	4.02
2.8	23.9617	6.9629	4.04

TABLE I: The analytic confirmation via numerics for the amplitudes of the tails at timelike infinity, where $\alpha = 0.03$ and $r = 5$.

We see that for all values of the initial amplitudes ε the value of decay rate γ is very close to the theoretical value. On the other hand, the analytical prediction for the amplitude is in excellent agreement with numerical data only for small initial data. For larger data this agreement disappears - this means that subleading terms with different dependance on the size of initial data are also important here.

For the comparison with numerical data it is convenient to define the local power index (hearafter LPI) defined as follows [10]:

$$n(t,r) = -t\frac{\dot{F}(t,r)}{F(t,r)}. \tag{39}$$

For the assumed form parametrising the tail (38) we get the following expression for the LPI:

$$n(t,r) = \gamma + \frac{B}{t} + \frac{2C}{t^2}. \tag{40}$$

In Fig. 2 we plot LPI at $r = 5$ as a function of $1/t$. All curves in this figure correspond to small initial data. We see that all lines approach the same power-law index $\gamma = 4$ at the future timelike infinity, so numerical data confirm analytical prediction for the decay rate.

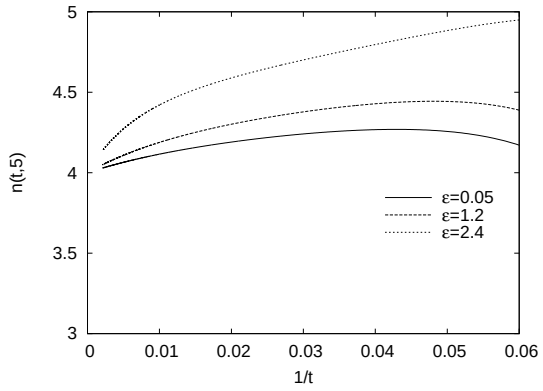

FIG. 2: The local power index n(t,5) as a function of 1/t.

In Fig 3 we plot $\epsilon^{-3}F(t,r)$ as a function of initial amplitude. According to the analytical prediction the late–time behaviour of this quantity does not depend on the magnitude of initial data. We may observe that for not-too-large initial data this is really the case.

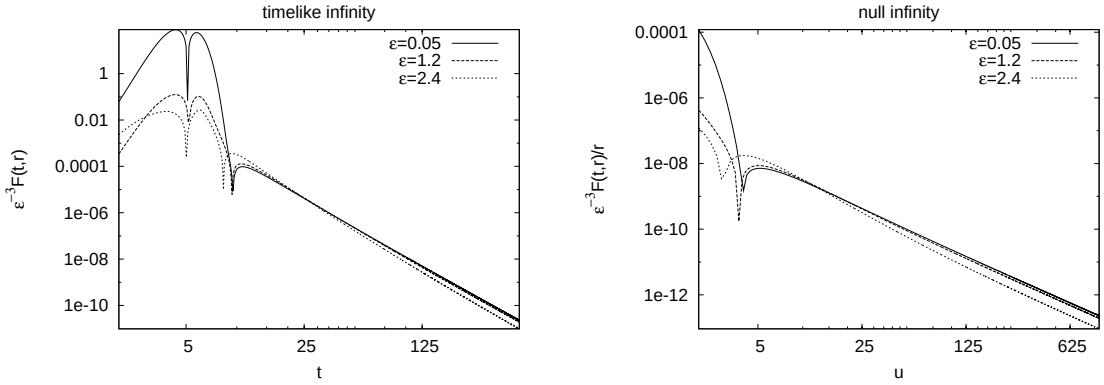

FIG. 3: Left panel: The log-log plot of $\epsilon^{-3}F(t,r)$ vs time for fixed r=5. Right panel: The log-log plot of $\epsilon^{-3}F(t,r)/r$ for fixed large advanced time $v = t + r = 1000$ as the function of retarded time $u = t - r$.

In Fig. 4 we plot the amplitude of the tail as a function of ϵ and α. For both panels the third-order estimation (solid lines) predicts correctly the amplitude of the tail for small data and fails for large data.

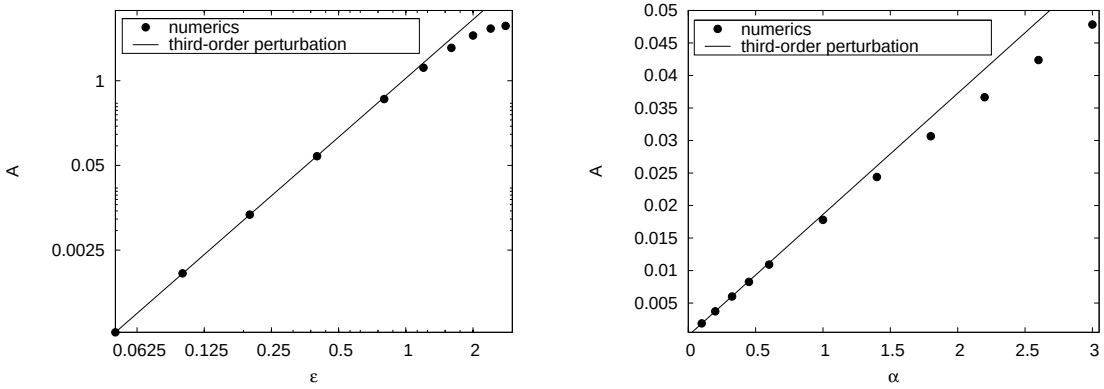

FIG. 4: Left panel: The log-log plot of the amplitude of the tail as a function of the amplitude of initial data for fixed $\alpha = 0.03$ and $r = 5$. Right panel: The plot of the amplitude of the tail as a function of the coupling constant α for fixed $\varepsilon = 0.08$ and $r = 5$.

Summary: Using *nonlinear* perturbation method, we derived explicit formulae for the late-time tail: the decay rate and the amplitude of a spherically symmetric, self-gravitating Einstein-Skyrme model. We showed that initial data decay as t^{-4} at the timelike infinity and as u^{-2} at future null infinity. Using third-order approximation we obtained analytical prediction for the amplitude that is in excellent agreement with numerics for sufficiently small initial data. For large data lying near the threshold of the black hole formation third-order approximation fails – it is seen in Fig. 4 in the deviation from the scaling $A \sim \varepsilon^3$ (left panel) and in the deviation from the linear dependence of A on α (right panel). Finally, we showed that the expression (34) describing the late-time tails in ES has the same form as the corresponding expression for the wave maps [4] .

Acknowledgments: I am greatly indebted to Andrzej Rostworowski and Tadeusz Chmaj for discussions and remarks. We acknowledge support by the MNII grants NN202 079235.

---

[1] Tadeusz Chmaj, private communication.
[2] Stanisław Zając, gr-qc/0906.4322
[3] P. Bizoń, T. Chmaj, and A. Rostworowski, math-ph/0701037
[4] P. Bizoń, T. Chmaj, A. Rostworowski and S. Zając, gr-qc/0906.2919
[5] P. Bizoń, T. Chmaj, and A. Rostworowski, Phys. Rev. D75, 121702(R) (2007).
[6] P. Bizoń, T. Chmaj, and A. Rostworowski, Class. Quantum Grav. 24, F55 (2007).
[7] P. Bizoń, T. Chmaj, and A. Rostworowski, Phys. Rev. D 76, 124035 (2007).
[8] P. Bizoń, T. Chmaj, and A. Rostworowski, Phys. Rev. D 78, 024044 (2008).
[9] T.H.R. Skyrme, Proc. R. Soc. **A260**, 127 (1961).
[10] L.M. Burko and A. Ori, Phys. Rev. D **56**, 7820 (1997).